Egypt. J. Chem. Vol. **68**, No.2, pp. 323 -331 (2025)

Egyptian Journal of Chemistry

http://ejchem.journals.ekb.eg/

Optimizing Oil Recovery with Eco-Friendly Biopolymer-Stabilized Aluminum Oxide Nanofluids: A Comparative Investigation of Egg and Soy Proteins

Amany A. Aboulrous [a*], M. M. Abdelhamid[a*], Philip Jaeger [b, c], and Eman Mostafa[a]

a Production department, Egyptian Petroleum Research Institute, Egypt
b Institute of Subsurface Energy Systems – ITE, Clausthal University of Technology, Germany
c Eurotechnica GmbH, Germany

Abstract
The increasing interest in employing nanofluids within the oil and gas sector has spurred significant research efforts. This study focuses on the formulation of two bio-nanofluids, comprising aluminum oxide nanoparticles suspended in isopropanol alcohol. Environmentally friendly dispersion stabilizers, namely egg and soy protein, were individually incorporated into the nanofluid formulations. The chemical composition and particle size distribution of the resulting nanofluids were rigorously characterized using X-ray diffraction (XRD) and dynamic light scattering (DLS) analyses, respectively.
Interfacial tension measurements between the bio-nanofluids and crude oil were conducted across a range of salinities, specifically 1, 3, and 5 wt.% NaCl solutions. Analysis of the oil recovery data revealed a notable improvement in performance with the soy protein-based nanofluid (SAO), exhibiting approximately a 36% enhancement in oil recovery at a concentration of 0.3 wt.% soy protein and 0.5 wt.% aluminum oxide nanoparticles and isopropanol. Similarly, the egg protein-based nanofluid (EAO) demonstrated a significant improvement of 33% in oil recovery at a concentration of 0.7 wt.% egg protein and 0.7 wt.% aluminum oxide nanoparticles and isopropanol. This discrepancy in performance was attributed to SAO's superior ability to reduce interfacial tension with crude oil, achieving a lower value of 0.03 mN/m compared to 0.04 mN/m for EAO at 3% NaCl.

Keywords: Protein; Nanoparticles; heavy oil recovery; oil production

1. Introduction

There is a rising need to improve the oil extraction methods from its reserves due to the increasing energy demand worldwide [1–2]. The used enhanced oil recovery (EOR) method depends majorly on the petrophysical properties of the rock, the composition of the hydrocarbon phase to be extracted and reservoir conditions [3–4]. One of the most important and used methods for oil extraction is chemical enhanced oil recovery (CEOR) because of its high recovery factor [4–5]. The surfactant flooding has gained attention as one of the most successful used CEOR methods [4]. The main mechanism of the surfactant flooding is lowering the interfacial tension (IFT) between crude oil and water and alter the wettability of the rock which leads to releasing the oil by decreased capillary forces in the porous medium [6]. However, the main challenges that surfactant flooding faces are surfactant adsorption on the rock which leads to increasing the cost of the process, and its harmful effect on the environment [7]. In order to solve these challenges, some authors reported using surfactant/alcohol mixtures to lower the interfacial tension using sulfonate/alcohol mixtures [8–12]. Lately, several authors reported using nanomaterials with different conventional enhanced oil recovery methods such as surfactant flooding [12–15], polymer flooding [16–18] and alkali/surfactant/polymer flooding [19–20] to enhance sweep efficiency by lowering the interfacial tension and altering the rock wettability. For instance, Xu et al. achieved low values of interfacial tension (IFT) between crude oil and formation water by using nanofluids (silica gel nanoparticles and an anionic surfactant) [21]. The lowest interfacial tension was achieved by using 0.05 wt % of the anionic surfactant. Suleimanov et al. used nanofluids which contain nonferrous metal nanoparticles and an anionic surfactant to lower IFT and enhance oil recovery [22].
In this study, the authors did not use brine to prepare the nanofluid. The lowest interfacial tension was reported at 0.001 wt % nanoparticle concentration. Shahzad et al. used different nanomaterials (silica, alumina, and zirconium oxide) and different types of surfactants to increase the oil recovery [23]. Concentrations of 0.01 wt % nanoparticles achieved the lowest interfacial tension (1.45 mN m−1) in there case. Moreover, Betancur et al. developed nanofluids that contain different cationic surfactants and silica gel nanoparticles. They studied the interactions between nanoparticles and surfactant; however, they didn't use brine to prepare nanofluids [24], the lowest interfacial tension (IFT) reaching down to 5 mN m−1. Betancur et al. improved oil

* Corresponding authors:.email**:** **mmahmoud.mohamed@gmail.com, (**M.M. Abdelhamid)
Receive Date: 02 April 2024,Revise Date: 07 May 2024, Accept Date: 21 July 2024
DOI: 10.21608/ejchem.2024.281127.9548

recovery by using a nanofluid which consists of a surfactant mixture and magnetic based carbon shell nanomaterials [25]. A concentration of 100 mg L−1 nanoparticles achieved the lowest interfacial tension. It is worth mentioning that these studies focused solely on effect of nanoparticles on the interfacial tension and not take into account the possibility of implementing synergistic effects by further compounds, e.g. in order to enhance the stability of the nanodispersion. Therefore, this study includes additional compounds next to aluminum oxide nanoparticles and isopropanol alcohol. As natural surfactant, proteins (egg and soy protein) were added, addressing a gap related to the exploration of multifunctional nanofluids. A comparative analysis for the two bio-nanofluids was made by using chemical flooding. Also, the interfacial tension properties of the bio-nanofluid were measured with crude oil, addressing the effect of different concentrations and optimizing conditions for enhanced oil recovery.

2. Experimental

2.1. Chemicals and materials

Egg protein and soy protein are supplied from local companies, while aluminum oxide nanoparticles (<50 nm particle size (DLS), 20 wt.% in isopropanol) (IA) are provided from Sigma-Aldrich. The characteristics of the investigated Egyptian crude oil are presented in Table 1.

Table 1 The characteristics of the investigated Egyptian crude oil

Characteristic	***API***	***aromatic***	***asphaltene***	***wax***	***resin***	***density***
Value, unit	18	43.6%	14.67 %	7.4%	24.87%	0.978 g/L

2.2. Bio-Nanofluid Preparation

In the first step, different concentrations of NaCl solution (1, 3, and 5 wt.%) were prepared. The investigated concentrations of aluminum oxide nanoparticles, which is 20 wt.% in isopropanol, were added to the brine solutions and stirred for half hour through a magnetic stirrer and then sonicated with an ultrasonic probe for two hours (25 kHz, 600 W). After that, different concentrations of egg protein and soy protein were separately introduced into the suspensions, and they were sonicated for another two hours. The particle size and zeta potential of the bio-nanofluids were measured by the Dynamic Light Scattering (DLS) using the Zetasizer Nano ZS instrument. The diffraction patterns of the prepared nanomaterials were determined by XRD analysis. X-ray diffraction (XRD) measurements were carried out using (Bruker D5005 XPERT) and CuKα radiation.

2.3. Surface, Interfacial and Wettability Measurements

The Surface tension measurements of the prepared bio-nanofluids, with different concentrations of protein and the same concentration of IA, were measured by De-Noüy Tensiometer (Kruss-K6 type) to determine the optimum concentration of protein in the bio-nanofluids, resulting in the lowest IFT between the bio-nanofluids and the investigated crude oil [7]. IFT is a useful indicator of the changes in capillary forces between oil and bio-nanofluids. When the IFT is reduced, it implies that the forces at the interface between oil and nanofluids are weakened.. By reducing IFT through the addition of bio-nanofluid, the capillary forces can be overcome more easily. This reduction in capillary forces is anticipated to enhance the efficiency of oil recovery processes [14–26]. The interfacial tension was measured by SDT (Kruss, Germany) while the contact angles were measured by Drop Shape Analyzer (Kruss, Germany). All Measurements were taken at room temperature.

2.4. Bio-Nanofluid Flooding Experiment

The flooding experiments were conducted using a sand-packed bed (589.28 ml total volume, 700 g mass of sand, 5.0 cm internal diameter and 30 cm in length). The porosity of the sand bed ranged between 24.9 and 26.32% and the sand size was of 0.70−1.75 mm (mesh size between 1.5 and 3.5 meshes). The sand bed was saturated with brine solution (NaCl: 30,000 ppm) for two days. Then, 150 ml of the investigated crude oil was injected at temperature 50 °C and pressure 2.0 MPa (reservoir conditions) at a flow rate of 1 cm3 / min, being left to be aged at 50 °C for a whole day. A secondary recovery was carried out by only brine solution (water flooding), and the oil recovery was measured at the end of this stage. Finally the bio-nanofluids were injected through the sand-packed setup under reservoir conditions with the same flow rate (1.0 cm3/min) [7–27]. The schematic setup for the flooding experiments is presented in Figure 1.

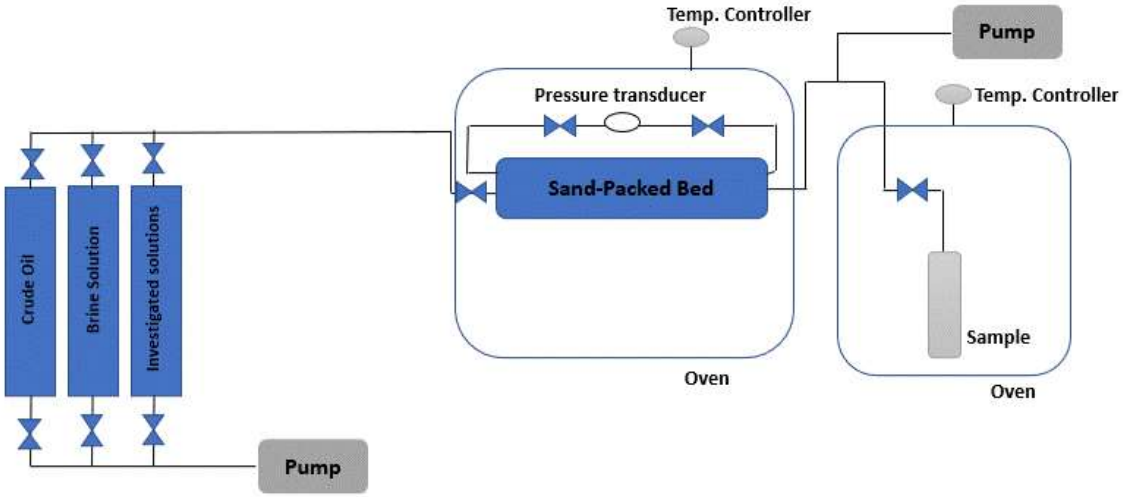

Figure 1 schematic of the used sand-packed bed for the bio-nanofluid flooding experiments.

3. Results and Discussion

3.1. Characterization of Bio-nanofluids

Figure 2 (A and B) shows the XRD pattern of soy protein (SAO) and egg protein (EAO) based nanofluids. For the pure protein, there are two diffraction peaks near °2θ of 9° and 19°, which are characteristic peaks of the α-helical and β-folded structures in the secondary structure of the protein, respectively [28–29]. Dipping Al2O3 nanoparticles to soybean and egg protein structures, it is a process of aggregation and entanglement between protein molecules; therefore, its molecular structure remains intact. The peak of protein widened and shifted to 19.5° after adding 20 wt% of Al2O3. This is because the Al2O3 disrupts the molecular structure of the protein and reacts with it by cross-linking [30–31]. The XRD exhibited characterization peaks of aluminum oxide (SAO and EAO) at scattering angles (2) of 25.8(3 0 0), 35.5◦ (4 0 1), 32.9◦(200), 38.1◦(104), 45.5(0 3 1),61.3◦, 67.1◦(214) and 90.1(119).

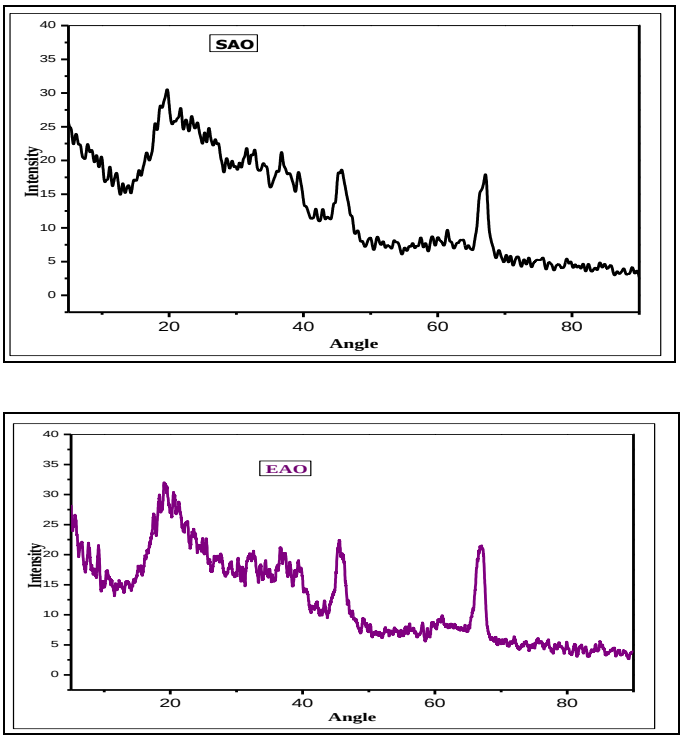

Figure 2 XRD pattern for SAO and EAO nanofluids

DLS also confirmed the nanosized particles of SAO and EAO. The size of SAO ranged from 37.84 to 78.82 nm, while the EAO ranged from 50.75 to 91.28 nm as shown in Table 2 and Figure 3.

Table 2 The particle size of the prepared nanofluids with distilled water

Compound		
Soy protein/Aluminum Oxide (SAO) nanofluid	43.82	- 42.3
Egg protein/Aluminum oxide (EAO) nanofluid	58.77	- 50.2

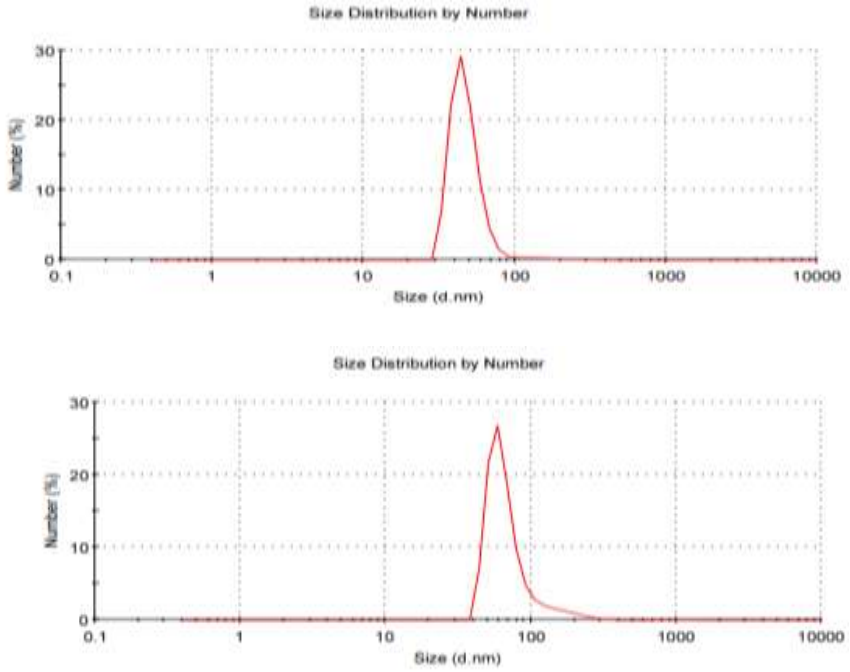

Figure 3 particle size distribution of SAO and EAO

3.2. Surface, Interfacial tension Measurements

In order to determine the optimum concentrations of protein at which the surface tension is the lowest within the nanofluid composition, five different concentrations of the protein (0.1, 0.3, 0.5, 0.7 and 1.0 wt.%) were investigated at the same concentration of aluminum oxide nanoparticles/isopropanol mixture (0.5 wt.%) in the nanofluids and a salinity (5 wt.% NaCl) as shown in Figure 4.

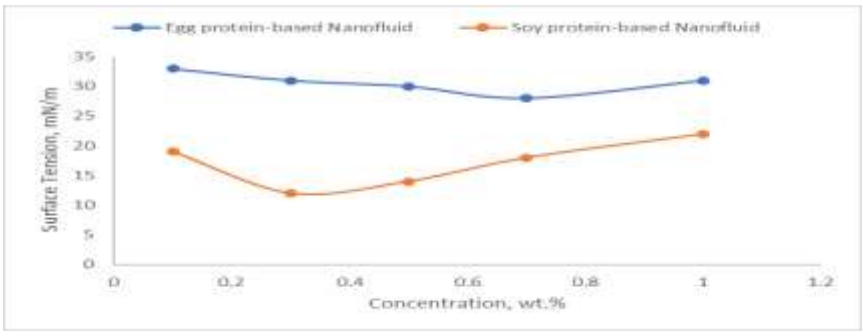

Figure 4 Surface tension for different concentrations of egg and soy protein at the same concentration of IA (0.5 wt.%) and 5 wt.% NaCl

At concentrations of 0.7 wt.%, egg protein, the lowest surface tension of the bio-nanofluid was found, while the soy protein achieved the lowest surface tension of bio-nanofluid at 0.3 wt.%. In the following, the surface tension for different concentrations of the mixture (aluminum oxide nanoparticles/isopropanol) were measured at different salinities (1, 3, and 5 wt.% NaCl), while keeping the concentration of the protein constant (0.7 wt.% for egg protein and 0.3 wt.% of soy protein) as seen in Figure 5.

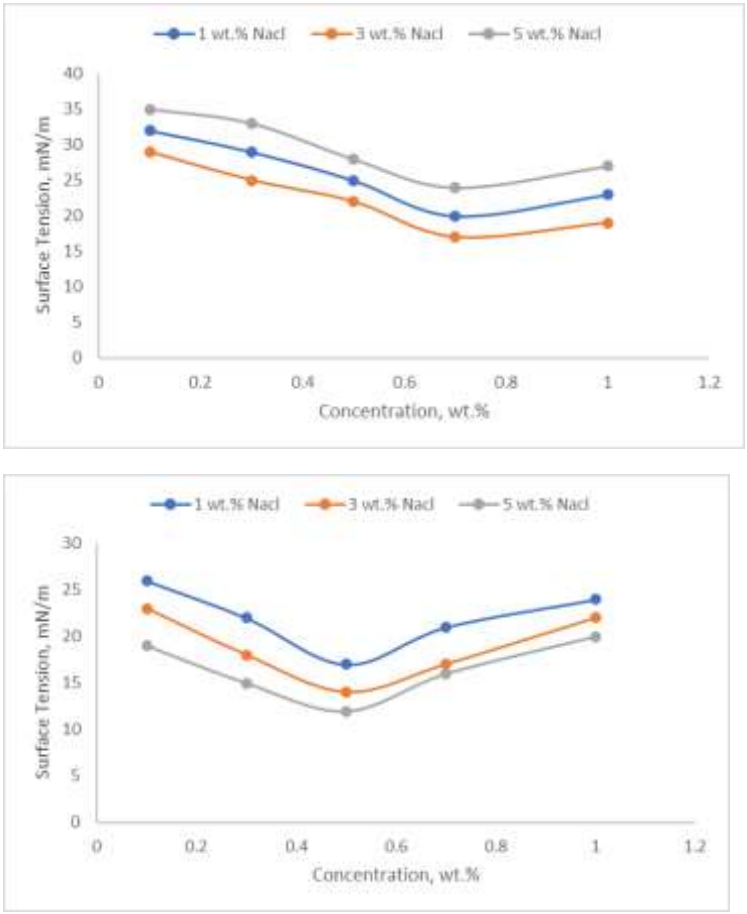

Figure 5 Surface tension for different concentrations of the mixture (aluminum oxide nanoparticles/isopropanol) with different proteins (a) Soy protein, and (b) Egg protein at different salinity (1, 3, and 5 wt.% NaCl)

The SAO exhibited the lowest surface tension at 0.5 wt.% of IA in the bio-nanofluid composition, while the EAO achieved the lowest value of surface tension at 0.7 wt.% of IA. The effect of increasing the content of salt was shown in Table 4. For ASO, the surface tension decreased with increasing salinity as it reached the lowest 12 mN/m at 5 wt.%.

While the surface tension decreased with increasing the salt to reach 17 mN/m at 3 wt.%, the surface tension increased by increasing the salt to 5 wt.% to be 24 mN/m. The amino acid composition and sequence of proteins can vary between soy and egg proteins. This can influence the overall molecular structure and interactions between protein molecules, affecting their ability to form cohesive forces at the surface.

For EAO nanofluids, this can be explained based on three mechanisms; (a) Water molecules are attracted to each other through hydrogen bonding. When salt is added, the ions (Na+ and Cl-) disrupt the hydrogen bonding network of water. The chloride ions can surround and shield the water molecules from each other. This disruption weakens the cohesive forces between water molecules, making it easier for the surface tension to decrease, (b) The ions from the salt can compete with water molecules for hydrogen bonding. Water molecules at the surface have fewer neighboring water molecules to bond with, and the presence of ions makes it less favorable for water-water interactions. This weakens the cohesive forces at the surface, leading to a reduction in surface tension, or (c) The addition of salt can increase disorder or entropy at the water-air interface. Water molecules at the surface are more ordered compared to those in the bulk, and the presence of salt disrupts this order. As a result, the surface tension decreases as the disorder at the interface increases.

Table 3 Interfacial tension of Bio-Nanofluids with crude oil (mN/m) at different concentrations of the mixture (aluminum oxide nanoparticles/isopropanol) at different salinity (1, 3, and 5 wt.% NaCl)

0.7 Egg protein with different concentration of IA			
0	26.39	22.8	17.4
0.3	0.1	0.07	0.19
0.5	0.08	0.05	0.12
0.7	0.05	0.04	0.08
1	0.09	0.06	0.1
0.3 Soy protein with different concentration of IA			
0	26.39	22.8	17.4
0.3	0.08	0.06	0.05
0.5	0.04	0.03	0.02
0.7	0.06	0.05	0.05
1	0.08	0.07	0.07

From Table 3, The lowest achieved interfacial tension for EAO nanofluid, with the investigated crude oil, was 0.04 mN/m at 0.7 wt.% egg protein and 0.7 wt.% of IA and salinity 3 wt.% NaCl, with increasing the salinity to 5 wt.%, the interfacial increased to 0.08 mN/m due to the complex structure of the egg protein. While the interfacial tension decreased from 17.4 mN/m to 0.02 mN/m by using 0.3 wt.% soy protein and 0.5 wt. % IA.

3.3. Wettability and Work of Adhesion

In Table 4, the change in wettability of the rock, i.e. in the contact angles are evaluated after the addition of the bio-nanofluids solutions. The contact angle changed from 153.45° to 26.8° 22.34° after the addition of the EAO (IA 0.7 wt.%) and SAO (IA 0.5 wt. %) respectively as shown in Table 4. The data showed that the rock wettability was changed from oil-wet to water-wet after the addition of the bio-nanofluids. Consequently, this lowered the adhesion forces between the rock surfaces and the oil drops which facilitate the displacement process of the oil recovery.

The bio-nanofluids are adsorbed at the sand rock surfaces leading to the repelling of the oil drops from the rock surface and further increasing the oil recovery [7–32]. Young-Dupre equation [32–33] measured the work of adhesion (Wa) by using the surface tension (YL) and the contact angle at the rocks surface (ɵ).

$$Wa = YL (1 + Cos (ɵ))$$

In table 4, the data of the work of adhesion is shown to decrease at increasing the bio-nanofluid concentration, achieving the lowest value at the smallest contact angle. The Wa decreased from the blank oil sample (3.5 mJ/m2) to 0.6702*10-3 mJ/m2 for SAO (0.5 wt. % of IA) nanofluid. The same behavior was observed for the EAO nanofluid (0.7 wt.% IA) as the lowest Wa was 1.0712* 10-3 mJ/m2. This confirms that the highest oil recovery is achieved at the lowest value for the adhesion work and the least IFT.

Table 4 Contact angle at different concentrations of IA, room temperature, and 3 wt.% NaCl

0.7 wt.% Egg protein		
Conc. (wt.%)	**Contact Angle (Ɵ)**	**Work of Adhesion (mJ/m^2)*10^{-3}**
0	153.45	3498.66
0.3	35.23	2.4661
0.5	32.45	1.6225
0.7	26.78	1.0712
1	34.72	2.0832
0.3 wt.% Soy protein		

Conc. (wt.%)	Contact Angle (Θ)	Work of Adhesion (mJ/m^2)*10^{-3}
0	153.45	3498.66
0.3	26.36	1.5816
0.5	22.34	0.6702
0.7	30.21	1.5105
1	33.64	2.3548

3.4. Oil Recovery by Bio-nanofluids Flooding

There are many factors that affect the flooding process such as the interfacial tension of the flooded solutions with the crude oil, and the wettability alteration of the rock surfaces. After the flooding with the bio-nanofluids, the interfacial tension between the crude oil and the injected bio-nanofluid changed the rock wettability to water-wet which consequently untrapped the oil from the rock pores. From the data listed in Table 5, the maximum oil recovery factor of 36.1% was achieved by 0.3 wt.% soy protein mixed with 0.5 wt. % IA. While the maximum oil recovery factor for egg protein based nanofluid was 33.5%, achieved with 0.7 wt. % egg protein and 0.7 wt. % IA. The difference between the incremental oil recovery factors of SAO and EAO nanofluids could be due to the difference between their chemical compositions. The molecular structure of proteins, including their amino acid composition and sequence, influences their interfacial behavior. Soy protein has a different amino acid composition and structure than egg protein, contributing to its superior interfacial properties. The specific arrangement of amino acids in soy protein allows for better adsorption and interaction at interfaces. Also, the hydrophobicity of a protein influences its ability to interact with oil droplets and form stable emulsions. Soy protein tends to have higher hydrophobicity compared to egg protein, which enhances its effectiveness at the oil-water interface, improving emulsion stability.

Table 5 Flooding Tests for Bio-nanofluids Using the Sand pack Model at 50 ºC.

Run No.	Initial oil Saturation %	Secondary Recovery %	Run Composition	Oil Recovery Factor %	Total Recovery %
1	87.9	32.4	0.7 wt. % egg protein + 0.3 wt. % IA	29.5	61.9
2	87.5	33.8	0.7 wt. % egg protein + 0.5 wt. % IA	31.5	65.3
3	88.3	34.2	0.7 wt. % egg protein + 0.7 wt. % IA	33.5	67.7
4	87.2	33.7	0.7 wt. % egg protein + 1.0 wt. % IA	29.7	63.4
5	88.1	34.5	0.3 wt. % soy protein + 0.3 wt. % IA	30.9	65.4
6	87.3	33.9	0.3 wt. % soy protein + 0.5 wt. % IA	36.1	70
7	87.7	33.5	0.3 wt. % soy protein + 0.7 wt. % IA	32.4	65.9
8	87.9	32.5	0.3 wt. % soy protein + 1.0 wt. % IA	31.8	64.3

4. Conclusion

In conclusion, the burgeoning interest in the application of nanofluids within the oil and gas industry has prompted the investigation of two bio-nanofluids in this study. These nanofluids were meticulously formulated through the amalgamation of aluminum oxide nanoparticles, isopropanol alcohol, and distinct additions of egg protein and soy protein. The chemical composition and particle dimensions of the resultant nanofluids were rigorously verified via X-ray diffraction (XRD) analysis and dynamic light scattering (DLS) analysis.

Interfacial tension measurements were conducted to assess the interactions between the examined bio-nanofluids and crude oil across varying salinities (1, 3, and 5 wt.% NaCl). The oil recovery outcomes demonstrated a notable enhancement, with the soy protein-based nanofluid (SAO) exhibiting a remarkable 36% improvement in oil recovery at concentrations of 0.3 wt.% soy protein, accompanied by 0.5 wt.% aluminum oxide nanoparticles and isopropanol. Similarly, the egg protein-based nanofluid (EAO) displayed a substantial 33% increase in oil recovery at concentrations of 0.7 wt.% egg protein, alongside 0.7 wt.% aluminum oxide nanoparticles and isopropanol.

The observed augmentation in oil recovery was attributed to the superior interfacial properties of SAO, as evidenced by a reduction in interfacial tension in contact with crude oil to 0.03 mN/m. In comparison, EAO achieved a lower interfacial tension of 0.04 mN/m at 3% NaCl. These findings underscore the potential of soy protein-based nanofluids as promising agents for enhanced oil recovery applications, emphasizing their favorable interfacial characteristics in comparison to their egg protein counterparts.

5. Conflicts of interest

There are no conflicts to declare.

6.Formatting of funding sources

List funding sources; Science, Technology & Innovation Funding Authority (STDF) under the grant ID (43961) titled "Utilization of new environmentally Friendly foaming systems based on nanomaterials in oil and gas production" and DAAD (ID: 57562255), within the framework of the German Egyptian Mobility Program for Scientific Exchange and Excellence Development (GE-SEED) Grant

7.Acknowledgements
The authors were supported by Science, Technology & Innovation Funding Authority (STDF) under the grant ID (43961) titled "Utilization of new environmentally Friendly foaming systems based on nanomaterials in oil and gas production" and the financial support from the DAAD (ID: 57562255), within the framework of the German Egyptian Mobility Program for Scientific Exchange and Excellence Development (GE-SEED) Grant.

8. References

1. S. Thomas, Enhanced Oil Recovery-An Overview Enhanced Oil Recovery-An Overview Molecular Structures of Heavy Oils and Coal Liquefaction Products Structure moléculaire des huiles lourdes et produits de liquéfaction du charbon. Oil & Gas Science and Technology-Rev. IFP, 63 (2008).
2. R. Al-Mjeni, S. Arora, P. Cherukupalli, J. Van Wunnik, J. Edwards, B. J. Felber, O. Gurpinar, G. J. Hirasaki, C. A. Miller, C. Jackson, M. R. Kristensen, F. Lim, & R. Ramamoorthy, Has the time come for EOR? Oilfield Review, 22 (2010).
3. T. Sharma, S. Iglauer, & J. S. Sangwai, Silica Nanofluids in an Oilfield Polymer Polyacrylamide: Interfacial Properties, Wettability Alteration, and Applications for Chemical Enhanced Oil Recovery. Industrial and Engineering Chemistry Research, 55 (2016). https://doi.org/10.1021/acs.iecr.6b03299.
4. mohammed, saja and Hadi, Nizar, Numerical and Experimental Study about Chemical Flooding by Polymer Towards Enhanced Oil Recovery (EOR): A review, Egyptian Journal of Chemistry, 2023, 66, 7, 603-619.
5. T. Sharma & J. S. Sangwai, Silica nanofluids in polyacrylamide with and without surfactant: Viscosity, surface tension, and interfacial tension with liquid paraffin. Journal of Petroleum Science and Engineering, 152 (2017). https://doi.org/10.1016/j.petrol.2017.01.039.
6. M. J. Rosen, H. Wang, P. Shen, & Y. Zhu, Ultralow interfacial tension for enhanced oil recovery at very low surfactant concentrations. Langmuir, 21 (2005). https://doi.org/10.1021/la0400959.
7. A. Mohamed Alsabagh, A. A. Aboulrous, M. Mahmoud Abdelhamid, T. Mahmoud, A. Sharifi Haddad, & R. Rafati, Improvement of Heavy Oil Recovery by Nonionic Surfactant/Alcohol Flooding in Light of the Alkane Carbon Number and Interfacial Tension Properties. ACS Omega, 6 (2021) 18668–18683. https://doi.org/10.1021/acsomega.1c01373.
8. N. Kumar & A. Mandal, Surfactant Stabilized Oil-in-Water Nanoemulsion: Stability, Interfacial Tension, and Rheology Study for Enhanced Oil Recovery Application. Energy and Fuels, 32 (2018). https://doi.org/10.1021/acs.energyfuels.8b00043.
9. M. El-Batanoney, T. Abdel-Moghny, & M. Ramzi, The effect of mixed surfactants on enhancing oil recovery. Journal of Surfactants and Detergents, 2 (1999). https://doi.org/10.1007/s11743-999-0074-7.
10. F. Comelles, J. Sánchez-Leal, & J. J. González, Influence of ionic surfactants on the formation of liquid crystals in oleic acid/glycol/water systems. Journal of Surfactants and Detergents, 10 (2007). https://doi.org/10.1007/s11743-007-1023-9.
11. J. L. Salager, A. M. Forgiarini, L. Márquez, L. Manchego, & J. Bullón, How to attain an ultralow interfacial tension and a three-phase behavior with a surfactant formulation for enhanced oil recovery: A Review. Part 2. performance improvement trends from Winsor's premise to currently proposed inter- and intra-molecular mixtures. Journal of Surfactants and Detergents, 16 (2013). https://doi.org/10.1007/s11743-013-1485-x.
12. J. L. Salager, A. M. Forgiarini, & J. Bullón, How to attain ultralow interfacial tension and three-phase behavior with surfactant formulation for enhanced oil recovery: A review. Part 1. Optimum formulation for simple surfactant-oil-water ternary systems. Journal of Surfactants and Detergents, 16 (2013). https://doi.org/10.1007/s11743-013-1470-4.
13. M. Zargartalebi, R. Kharrat, & N. Barati, Enhancement of surfactant flooding performance by the use of silica nanoparticles. Fuel, 143 (2015). https://doi.org/10.1016/j.fuel.2014.11.040.
14. G. Cheraghian & L. Hendraningrat, A review on applications of nanotechnology in the enhanced oil recovery part A: effects of nanoparticles on interfacial tension. International Nano Letters, 6 (2016). https://doi.org/10.1007/s40089-015-0173-4.
15. Y. Wu, W. Chen, C. Dai, Y. Huang, H. Li, M. Zhao, L. He, & B. Jiao, Reducing surfactant adsorption on rock by silica nanoparticles for enhanced oil recovery. Journal of Petroleum Science and Engineering, 153 (2017). https://doi.org/10.1016/j.petrol.2017.04.015.
16. L. J. Giraldo, M. A. Giraldo, S. Llanos, G. Maya, R. D. Zabala, N. N. Nassar, C. A. Franco, V. Alvarado, & F. B. Cortés, The effects of SiO2 nanoparticles on the thermal stability and rheological behavior of hydrolyzed polyacrylamide based polymeric solutions. Journal of Petroleum Science and Engineering, 159 (2017). https://doi.org/10.1016/j.petrol.2017.10.009.
17. A. Rezaei, M. Abdi-Khangah, A. Mohebbi, A. Tatar, & A. H. Mohammadi, Using surface modified clay nanoparticles to improve rheological behavior of Hydrolized Polyacrylamid (HPAM) solution for enhanced oil recovery with polymer flooding. Journal of Molecular Liquids, 222 (2016). https://doi.org/10.1016/j.molliq.2016.08.004.
18. D. Zhu, L. Wei, B. Wang, & Y. Feng, Aqueous hybrids of silica nanoparticles and hydrophobically associating hydrolyzed polyacrylamide used for EOR in high-temperature and high-salinity reservoirs. Energies, 7 (2014). https://doi.org/10.3390/en7063858.
19. J. A. Ali, K. Kolo, A. K. Manshad, & A. H. Mohammadi, Recent advances in application of nanotechnology in chemical enhanced oil recovery: Effects of nanoparticles on wettability alteration, interfacial tension reduction, and flooding. Egyptian Journal of Petroleum, 27 (2018). https://doi.org/10.1016/j.ejpe.2018.09.006.
20. K. Rahimi, M. Adibifard, M. Hemmati, H. Shariat Panahi, & S. Gerami, Experimentally investigation of the effects of nanoparticles-enriched ASP formulations on the spontaneous imbibition in a fractured sandstone reservoir. Asia-Pacific Journal of Chemical Engineering, 11 (2016). https://doi.org/10.1002/apj.1947.
21. D. Xu, B. Bai, Z. Meng, Q. Zhou, Z. Li, Y. Lu, H. Wu, J. Hou, & W. Kang, A novel ultra-low interfacial tension nanofluid for enhanced oil recovery in super-low permeability reservoirs. Soc. Pet. Eng. - SPE Asia Pacific Oil Gas Conf. Exhib. 2018, APOGCE 2018 (2018). https://doi.org/10.2118/192113-ms.

22. B. A. Suleimanov, F. S. Ismailov, & E. F. Veliyev, Nanofluid for enhanced oil recovery. Journal of Petroleum Science and Engineering, 78 (2011) 431–437. https://doi.org/10.1016/J.PETROL.2011.06.014.
23. M. S. Kamal, A. A. Adewunmi, A. S. Sultan, M. F. Al-Hamad, & U. Mehmood, Recent advances in nanoparticles enhanced oil recovery: Rheology, interfacial tension, oil recovery, and wettability alteration. Journal of Nanomaterials, 2017 (2017). https://doi.org/10.1155/2017/2473175.
24. S. Betancur, F. Carrasco-Marín, C. A. Franco, & F. B. Cortés, Development of Composite Materials Based on the Interaction between Nanoparticles and Surfactants for Application in Chemical Enhanced Oil Recovery. Industrial and Engineering Chemistry Research, 57 (2018). https://doi.org/10.1021/acs.iecr.8b02200.
25. S. Betancur, F. Carrasco-Marín, A. F. Pérez-Cadenas, C. A. Franco, J. Jiménez, E. J. Manrique, H. Quintero, & F. B. Cortés, Effect of Magnetic Iron Core-Carbon Shell Nanoparticles in Chemical Enhanced Oil Recovery for Ultralow Interfacial Tension Region. Energy and Fuels, 33 (2019). https://doi.org/10.1021/acs.energyfuels.9b00426.
26. F. B. Cortés, M. Lozano, O. Santamaria, S. B. Marquez, K. Zapata, N. Ospina, & C. A. Franco, Development and evaluation of surfactant nanocapsules for chemical Enhanced Oil Recovery (EOR) applications. Molecules, 23 (2018). https://doi.org/10.3390/molecules23071523.
27. N. A. Samak, T. Mahmoud, A. A. Aboulrous, M. M. Abdelhamid, & J. Xing, Enhanced Biosurfactant Production Using Developed Fed-Batch Fermentation for Effective Heavy Crude Oil Recovery. Energy & Fuels, 34 (2020) 14560–14572. https://doi.org/10.1021/acs.energyfuels.0c02676.
28. J. Chen, X. Chen, Q. Zhu, F. Chen, X. Zhao, & Q. Ao, Determination of the domain structure of the 7S and 11S globulins from soy proteins by XRD and FTIR. Journal of the Science of Food and Agriculture, 93 (2013). https://doi.org/10.1002/jsfa.5950.
29. E. M. Mostafa & E. Amdeha, Enhanced photocatalytic degradation of malachite green dye by highly stable visible-light-responsive Fe-based tri-composite photocatalysts. Environmental Science and Pollution Research, 29 (2022). https://doi.org/10.1007/s11356-022-20745-6.
30. X. Li, Y. Zhou, J. Li, K. Li, & J. Li, Perm-Inspired High-Performance Soy Protein Isolate and Chicken Feather Keratin-Based Wood Adhesive without External Crosslinker. Macromolecular Materials and Engineering, 306 (2021). https://doi.org/10.1002/mame.202100498.
31. J. Gangwar, K. K. Dey, Komal, Praveen, S. K. Tripathi, & A. K. Srivastava, Microstructure, phase formations and optical bands in nanostructured alumina. Advanced Materials Letters, 2 (2011). https://doi.org/10.5185/amlett.2011.3233.
32. A. H. Ayyad, Thermodynamic derivation of the Young–Dupré form equations for the case of two immiscible liquid drops resting on a solid substrate. Journal of Colloid and Interface Science, 346 (2010) 483–485. https://doi.org/10.1016/J.JCIS.2010.03.044.
33. M. E. Schrader, Young-Dupre Revisited. *Langmuir*, 11 (2002) 3585–3589. https://doi.org/10.1021/la00009a049.